

### Review

# Surface chemistry of hydroxyapatite for sustainable *n*-butanol production from bio-ethanol

Daniyal Kiani<sup>1,\*</sup> and Jonas Baltrusaitis<sup>1,\*</sup>

#### **SUMMARY**

Calcium hydroxyapatite (HAp) has emerged as a green, bifunctional catalyst for the heterogeneous coupling of various biomass-derived molecules, including ethanol to *n*-butanol via the Guerbet reaction. This review critically analyzes the surface chemistry of HAp catalysts based on the available temporally- and spatially-resolved *in situ* and *operando* spectroscopic studies. Specifically, the nature of the isolated acidic and basic surface sites, as well as the acid-base pairs, is elucidated based on chemical probe spectroscopy results. Surface structure-reactivity relationships are also rationalized based on the nature and identity of the surface sites involved in various steps of the Guerbet reaction to produce *n*-butanol over the HAp catalysts. Finally, future directions in experimental investigations are suggested to guide the rational design of improved HAp-based catalysts for the Guerbet reaction and other similar chemistries.

### INTRODUCTION

Despite significant advancements in converting biomass-derived hydrocarbon and oxygenate feedstock, their commercial adoption has been slow because of both economic and technological barriers. Utilizing a diverse range of renewable feedstock comes with significant advantages, including the ability to respond to market demand fluctuations and maximize profits of the plant over the lifetime. While government incentives have stimulated the use of bio-feedstock, significant advancements in catalyst design, process development, and intensification are still necessary to expand and integrate these bio-feedstocks to synthesize high-value fuels and chemicals. One of the most important and widely produced bio-feedstock molecules is bio-ethanol. Bio-ethanol production capacity was over 27 billion gallons/ year worldwide in 2016, of which the US produced over 15 billion gallons. 1 Its primary use is in blending with gasoline, accounting for 90% of bio-ethanol demand.<sup>1</sup> Bio-ethanol can be obtained from biomass resources by fermentation of a range of raw materials, such as corn, sugarcane, and lignocellulose.<sup>2</sup> Provided the limit on the maximum ethanol blend level in gasoline and the increase in bio-ethanol production capacity, there is an opportunity to utilize renewable bio-ethanol as a platform chemical to catalytically convert it to value-added fuels and chemicals, such as butanol ( $C_4H_9OH$ ). Unlike ethanol ( $C_2H_5OH$ ),  $C_4H_9OH$  can be used not only as a fuel additive but also as a fuel directly, given its higher volumetric energy content (26.7 MJ/L), and low heating value basis.<sup>3,4</sup> Other advantages offered by n- $C_4H_9OH$  over  $C_2H_5OH$  include that it is immiscible in water and has a lower Reid vapor pressure (i.e., lower volatility and evaporative emissions), making it safer and more economical to process/handle.<sup>4,5</sup> Moreover, C<sub>4</sub>H<sub>9</sub>OH has been reported to lower SO<sub>x</sub> and NO<sub>x</sub> engine emissions in mixtures when compared with gasoline.<sup>5</sup>

### The bigger picture

Catalytic conversion of biomassderived molecules is an essential route for renewable chemical and fuel synthesis as the chemicals industry transitions from fossil fuel-derived hydrocarbons toward more sustainable feedstocks. Understanding the catalyst surface chemistry is of paramount importance for the accelerated development of structure-activity/ selectivity relationships that form the basis for the rational design and optimization of catalysts at large. Here, we highlight the state-of-the-art understanding regarding the surface chemistry of hydroxyapatite (HAp)—a catalyst that enables the production of value-added alcohols from bioethanol. Given the current state of understanding and the future roadmap provided in this review, we expect this field to progress into a mature, productive avenue for the rational design and application of HAp-based catalysts for various acid-basecatalyzed chemistries, including the Guerbet reaction of ethanol to n-butanol.



The material compatibility problems are also substantially less severe for  $C_4H_9OH$  than  $C_2H_5OH$ , with little or no reported swelling of elastomers and a lower corrosivity toward ferrous metals. Finally, under the Renewable Fuel Standard,  $^6C_4H_9OH$  also meets the renewable fuel 20% greenhouse gas emission reduction threshold, making it an extremely lucrative target molecule.  $^{4,6}$ 

Hallmarks of an effective *green* catalyst include (1) its synthesis via green chemistry techniques that preclude the use of toxic chemicals and solvents, (2) high selectivity, (3) improvement in the overall reaction atom efficiency, and (4) enabling solvent-free product synthesis. In addition, the catalyst needs to satisfy the basic requirements of high recyclability, stability, and availability. Hydroxyapatite (HAp) is a material that naturally occurs in igneous rock, animal bones, and teeth. Although in its mineral form it can be easily mistaken with more precious stones, such as beryl, amethyst, or olivine, a drop of lime juice is enough to start dissolving it—the reason for which A.G. Werner named it in 1786 using the Greek word " $\alpha\pi\alpha\tau\alpha\sigma$ ," meaning "to deceive" or "to mislead." Recently, HAp has also emerged as one of the greenest, bio-compatible catalysts of high industrial value because of its unique bifunctional properties and ion-exchange capabilities. While HAp can be sourced naturally, it is synthesized via a simple co-precipitation method for catalytic applications to ensure control over composition, structure, and purity.

The stoichiometric formula of HAp is  $Ca_{10}(PO_4)_\delta(OH)_2$ , where the molar Ca/P ratio is 1.67. A deviation from this stoichiometry by varying the Ca/P ratio in the range of 1.50–1.80 offers non-stoichiometric HAp, which allows tailoring the surface acid-base chemistry and the resulting catalytic properties. Often, the presence of a mixture of several calcium phosphate phases was reported as one of the possible explanations for varying Ca/P ratios different from 1.67. Nowever, it has been recently demonstrated that is indeed possible to vary the Ca/P ratio in clean, well-crystallized HAp samples in the absence of other calcium phosphate phases by changing synthesis pH conditions. In terms of bulk crystalline structure, HAp crystallizes in either the monoclinic or hexagonal crystal systems. The monoclinic HAp (space group  $P2_1/b$ ) the most ordered, stoichiometric, and thermodynamically stable form of HAp, which can be obtained only at very high temperatures. Hexagonal HAp, on the other hand, belongs to the  $P6_3/m$  space group and may be non-stoichiometric.

Over the past two decades, HAp has emerged as a green catalyst for bio-feedstock conversion, as seen from the most used keywords in the bibliometric network analysis in Figure 1. Based on 221 literature reports, the network analysis suggests that HAp is finding increased use as a catalyst for chemistries relevant to bio-feedstock upgradation, especially for C–C bond coupling of alcohols via the Guerbet reaction, <sup>11,17–25</sup> Michael addition, <sup>26</sup> and aldol condensation. <sup>9,27–29</sup>

While excellent reviews on bio-feedstock relevant chemistries, such as the Guerbet reaction  $^{17,22}$  to produce n-C<sub>4</sub>H<sub>9</sub>OH from C<sub>2</sub>H<sub>5</sub>OH, are available in the literature, few reviews focus on the relevant surface chemistry of the HAp catalysts. Therefore, this review aims to provide a thorough understanding of the HAp surface chemistry and structural dynamics that ultimately make it an effective catalyst for C<sub>2</sub>H<sub>5</sub>OH coupling, based on state-of-the-art *in situ* and *operando* characterization techniques, including infrared (IR) spectroscopy, chemical probe IR studies, nuclear magnetic resonance (NMR), X-ray photoelectron spectroscopy (XPS), and ion scattering spectroscopy (ISS). This review is dedicated to critically analyzing the most advanced, recent literature pertaining to HAp's surface chemistry toward n-C<sub>4</sub>H<sub>9</sub>OH production

<sup>&</sup>lt;sup>1</sup>Department of Chemical & Biomolecular Engineering, Lehigh University, Bethlehem, PA 18015. USA

<sup>\*</sup>Correspondence: dak517@lehigh.edu (D.K.), job314@lehigh.edu (J.B.)

https://doi.org/10.1016/j.checat.2021.06.005

Review



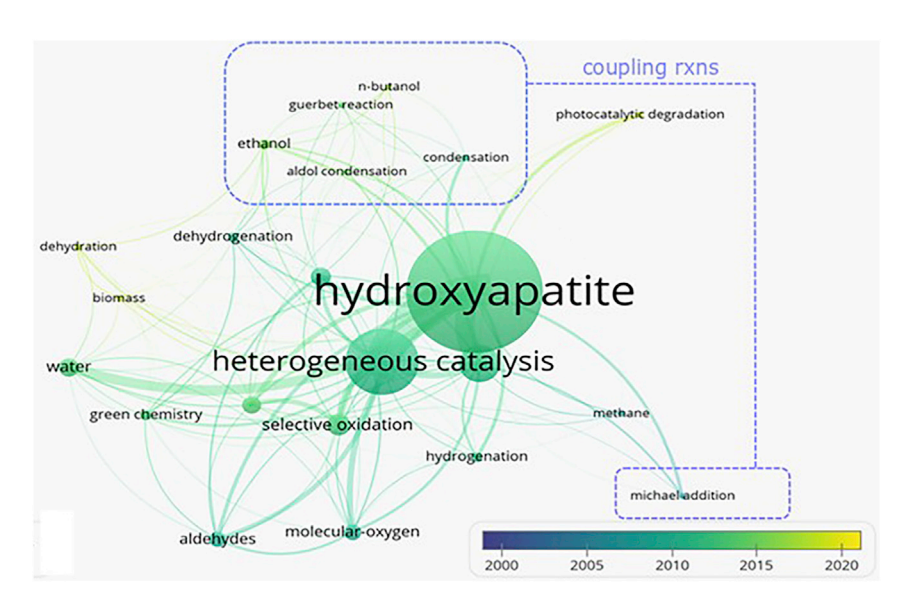


Figure 1. The bibliometric network of "hydroxyapatite catalysis" literature.

This analysis was comprised of 221 reports from the past 2 decades, downloaded from Web of Science in November 2020, generated by VOSviewer.

The network was analyzed for keywords occurring at least 5 times. It can be seen that the use of HAp as a heterogeneous catalyst significantly increased around 2010, and typically includes its application in bio-feedstock chemistry, including bond coupling reactions, such as aldol condensation, Michael addition, and the Guerbet reaction. Some literature reports are also present that utilize HAp for hydrocarbon oxidation or dehydrogenation.

from  $C_2H_5OH$  to generate structure-performance relationships and highlight avenues for further research. For a broader materials perspective, the reader is directed to existing reviews on HAp synthesis, properties, and applications. <sup>30,31</sup>

### SURFACE STRUCTURE OF HAP

The Ca/P ratio in HAp cannot be set by adjusting the molar concentrations of Ca and P precursors during synthesis only; this is because the Ca/P ratio also depends on how many structural carbonates incorporate into the HAp lattice from ambient  $CO_2$  dissolving into the precursor solution during synthesis.  $^{10,32-34}$  Also, the Ca/P ratio in the bulk of the material does not account for the OH<sup>-</sup> concentration that is known to be influenced by the presence of structural defects.  $^{32}$  Therefore, a more accurate chemical description for HAp found in the literature is summarized as  $Ca_{10-x-B}(PO_4)_{6-x-B}(HPO_4)_x(CO_3)_{A+B}(OH)_{2-x-2A-B}$ , where A and B are related to carbonates located in OH<sup>-</sup> and  $H_xPO_4^{(3-x)}$  structural sites, respectively.  $^{32}$ 

Despite the lack of understanding regarding the effects of bulk composition (i.e., Ca/P ratio, defects, etc.) on the surface composition and structure of HAp, pioneering work in the HAp catalysis literature does provide empirical structure-function relationships in this regard. Specifically, it has been shown that changing the Ca/P bulk ratio during HAp synthesis leads to a systematic change in the kinetics of the various acid- or base-catalyzed steps involved in the reaction mechanism (e.g., in the Guerbet reaction), which was attributed to changes in the density of acidic and basic surface sites with varying the Ca/P ratio. However, direct experimental evidence of how the bulk Ca/P ratio effects the surface composition, structure, site density, nature of surface sites, etc., is yet to be revealed. Provided that HAp can contain carbonate, phosphate, and hydroxyl groups, both in the bulk and on the surface, the discrimination between bulk and surface species remains challenging, yet critical, to advancing HAp catalysis. Therefore, the



# Chem Catalysis Review

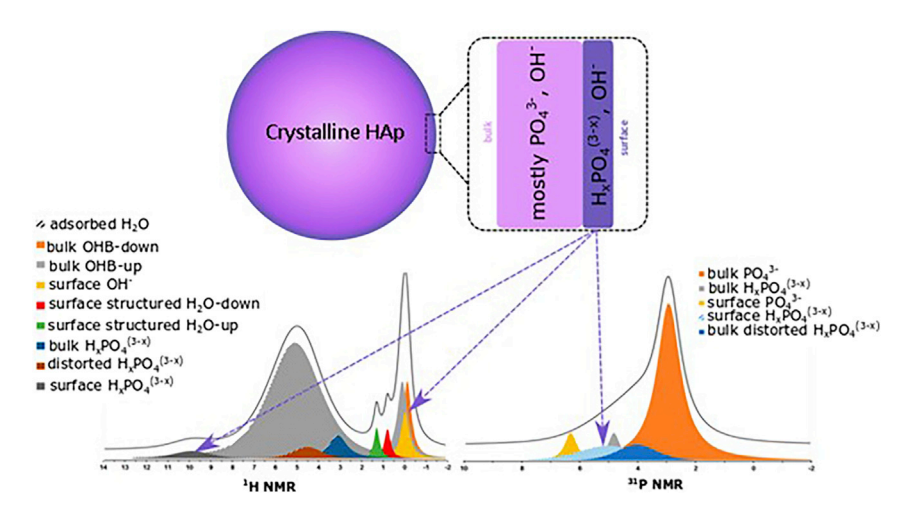


Figure 2. MAS NMR (<sup>1</sup>H and <sup>31</sup>P) of HAp catalysts.

MAS-NMR results indicate that the HAp surface is comprised of OH  $^-$  and  $\rm H_xPO_4^{(3-x)}$ , and  $\rm PO_4^{3-}$  sites.

Note that the NMR intensities of the different contributions are not directly representative of their concentration. MAS-NMR adapted from Ben Osman et al.  $^{36}$ 

following sub-sections attempt to elucidate the HAp surface structure and composition critical to understanding the active surface sites involved in acid-base catalysis, including Guerbet reaction.

#### Solid-state NMR

NMR-based techniques have widely been utilized to study various structural aspects of HAp.  $^{43}$ Ca solid-state NMR studies have shown that Ca exists as two distinct sites in HAp; Ca(I) and Ca(II), where the Ca(I)/Ca(II) ratio was  $\sim$ 0.67.  $^{35}$  It was hypothesized that Ca(I) could be either 6 or 9 coordinated with an average Ca-O length of 2.43 or 2.55 Å, respectively.  $^{35}$  On the other hand, Cal(II) could be 4, 6, or 7 coordinated, with an average Ca-O length of 2.37, 2.41, or 2.46 Å.  $^{35}$  However, the authors did not attempt to discriminate between bulk versus surface Ca sites. Also note that  $^{43}$ Ca NMR cannot be used to characterize a sample without previous  $^{43}$ Ca enrichment.

While some examples of <sup>43</sup>Ca NMR are present in the literature, most literature studies have focused on <sup>1</sup>H and <sup>31</sup>P NMR. As summarized in Figure 2, by using 2D solid-state <sup>1</sup>H and <sup>31</sup>P MAS-NMR, it was confirmed that the surface of the well-crystallized HAp particles with varying Ca/P ratio pretreated at 623 K under vacuum terminated in mostly protonated-phosphate groups,  $H_xPO_4^{(3-x)}$  (x = 0-2), with a minor population of PO<sub>4</sub> <sup>3-.36</sup> On the other hand, the bulk structure mostly contained PO<sub>4</sub><sup>3-</sup> groups in the 3D HAp framework. <sup>36</sup> However, defective HPO<sub>4</sub><sup>2-</sup> species were also identified in the bulk, <sup>36</sup> and it was hypothesized that carbonate impurities were responsible for the symmetry perturbation of these protonated-phosphate groups. <sup>36</sup> Via controlled synthesis to adjust bulk Ca/P ratios, authors also observed the dependence of relative intensities of the various MAS-NMR contributions corresponding to various bulk and surface hydrogen and phosphorous-containing species on the stoichiometry  $Ca_{10-x}(PO_4)_{6-x}(HPO_4)_x(OH)_{2-x}$ . Moreover, a peculiar feature of HAp surface, as it was exposed to ambient conditions, was also observed in the NMR study; the authors not only identified the well-known broad NMR signal associated with water adsorbed on surface  $Ca^{2+}$  and  $H_xPO_4^{(3-x)}$  but also unique signals due to structured water molecule stacking along the vertical axis in continuation with the internal OH<sup>-</sup> channels.<sup>36</sup> MAS-NMR studies elsewhere in the literature

Review



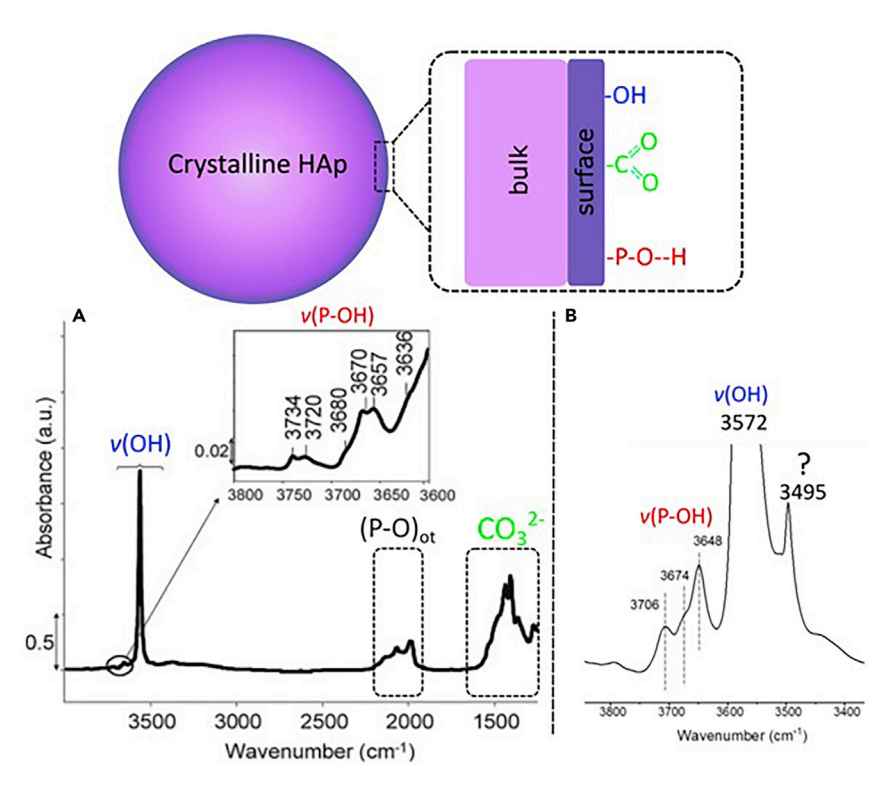


Figure 3. In situ IR spectra of HAp catalysts

IR spectra of HAp catalysts exhibit peaks in three main regions: 3,400–4,000 cm<sup>-1</sup> region with various peaks from O-H groups, the 1,900–2,100 cm<sup>-1</sup> region with P-O overtones, and the 1,300–1,600 cm<sup>-1</sup> region with different C-O bands due to carbonates. Figures were adapted from (A) Diallo-Garcia et al., <sup>40</sup> copyright American Chemical Society and (B) supplemental information of Wang et al., <sup>19</sup> copyright John Wiley and Sons.

demonstrated that, even at 800°C, adsorbed water was still present on the HAp surface.<sup>37</sup> The unique ability of HAp surface sites to stack water molecules and their propensity to hydrate may be of importance to understanding the surface chemistry of HAp-catalyzed reactions since water is involved in those reactions (*vide infra*).

### In situ IR spectroscopy

The structure of HAp has been characterized by vibrational spectroscopies in various modes, including transmission and diffuse reflectance. 19,38,39 Specifically, in situ IR spectroscopy of dehydrated HAp samples exhibited three major IR active regions, <sup>19,38,39</sup> as summarized in Figure 3A: the 3,400-4,000 cm<sup>-1</sup> region with various peaks from O-H groups, the 1,900-2,100 cm<sup>-1</sup> region with P-O overtones, and the 1,300-1,600 cm<sup>-1</sup> region with different C-O bands due to carbonate impurities. The most informative region from a catalysis perspective to understand the nature of surface functional groups is the 3,400–4,000 cm<sup>-1</sup> region. In this IR region, all studies reported a sharp, intense peak at 3,572 cm<sup>-1</sup> associated with bulk and surface OH groups. 19,39 Using C<sub>2</sub>H<sub>2</sub> adsorption, and isotope-labeling studies, it was shown that the 3,572 cm<sup>-1</sup> peak decreased upon probe molecule adsorption, indicating that there is a contribution from surface OH groups in this peak as well.<sup>38,40</sup> According to isotopically labeled HAp analysis via IR spectroscopy, the 3,636, 3,670, 3,680, 3,720, and 3,734 cm<sup>-1</sup> peaks correspond to the surface P-OH groups, while the 3,657 cm $^{-1}$  peak belongs to bulk  $H_xPO_4^{(3-x)}$ . $^{40}$  Across various studies, the ratio of surface-to-bulk P-OH vibrations and the exact IR peak positions is expected to vary depending on the sample synthesis procedure, temperature, and the gaseous environment utilized in the study.



Interestingly, a sharp peak at  $\sim 3,500 \text{ cm}^{-1}$  is also observed in some reports for stoichiometric HAp (Ca/P = 1.67). <sup>19</sup> This sharp peak at  $\sim$  3,500 cm<sup>-1</sup> is marked with a "?" in Figure 3B as it has not been assigned, according to the best of our knowledge. Due to the lower wavenumber position of this peak relative to other O-H peaks discussed above, and its narrow shape, it can be hypothesized that this  $\sim$ 3,500 cm<sup>-1</sup> peak belongs to isolated O-H groups that are acidic (i.e., the O-H bond is weaker than other O-H groups that vibrate at higher wavenumbers), although its exact origin and spatial location, e.g., surface versus bulk, remains unclear. As this peak has largely remained neglected in other IR characterization studies (zoomed-in spectra in this region are not always available), its involvement in the catalytic mechanism over HAp is still not well understood. At a similar position of  $\sim$ 3,534 cm<sup>-1</sup>, a peak was reported in a different study and attributed to O-H groups formed as a result of thermal treatment of the HAp catalyst.<sup>32</sup> Moreover, it should be noted that bicarbonates  $(H_xCO_3^{(2-x)})$  can also exhibit an IR peak at  $\sim$ 3,500 cm<sup>-1</sup> from C-O-H,<sup>41</sup> and thus the possibility of the IR peak in the  $\sim$ 3,500 cm<sup>-1</sup> region being the O-H vibration from surface bicarbonate needs to be entertained, and the contribution of such surface H<sub>x</sub>CO<sub>3</sub><sup>(2-x)</sup> sites toward Hap-catalyzed reaction investigated.

To the best of our knowledge, in situ/operando temperature-programmed desorption (TPD) IR studies (especially in diffused reflectance mode) are not available that could spectro-kinetically elucidate the dynamic evolution of peaks corresponding to various surface OH groups (i.e., P-OH, Ca-OH, C-OH, etc.) as a function of environmental conditions (temperature, gas) and exposure to reaction relevant molecules, such as  $C_2H_5OH$ ,  $H_2O$ , etc. Specifically, in situ spectroscopic studies can reveal the evolution of surface OH sites from in situ hydroxylation/dehydroxylation during  $C_2H_5OH$  coupling, where  $H_2O$  forms as a by-product. Since the degree of hydroxylation of heterogeneous catalytic materials is a key parameter to tune their reactivity, further temporally resolved in situ/operando IR studies are required to fully understand the surface chemistry and reactant-surface interactions of each kind of surface site to ascertain their role toward the reaction.

### Surface and sub-surface composition of HAp using XPS and ISS

The surface structure and composition of crystalline materials in general  $^{42-45}$  and HAp $^{46}$  in particular are known to differ significantly from the bulk. Preliminary evidence of structural and compositional variation between the surface and sub-surface HAp was obtained using molecular dynamics, which showed that, during thermal treatment, the surface underwent significant restructuring due to OH $^-$  ions migrating outward from the bulk to the surface and bonding with the outer Ca $^{2+}$  ions.  $^{47,48}$  The phosphate groups then occupy the holes left by the hydroxyls in the bulk layer. The hydroxyl surface enrichment also leads to a decrease in Ca $^{2+}$  electrophilicity.  $^{47,48}$  Moreover, the terminal OH groups from restructuring were suggested to lower the surface energy, making it a thermodynamically favorable process.  $^{49}$ 

Very recently, experimental evidence has emerged that corroborates the Ca enrichment of the surface in HAp.  $^{46}$  As depicted in Figure 4, the Ca/P ratio in the amorphous surface layer (top one to three atomic layers; 1 nm) was found to be  $\sim\!\!7$ —much higher than the bulk stoichiometric Ca/P ratio of 1.67.  $^{46}$  Semi-quantitative results from ISS also showed that the HAp surface was comprised of 83.5% Ca, 12.5% P, 1.5% O, and 2.5% C (due to carbonate adsorption).  $^{46}$  Fundamentally, the reason for this Ca enrichment in HAp and other calcium phosphates is not well understood. It was hypothesized that Ca $^{2+}$  has lower hydration energy than PO $_{4}^{3-}$  and, in environments where HAp interfaces with water, there may be thermodynamic benefits from having Ca $^{2+}$  occupy sites in the topmost atomic layer of the

**Review** 



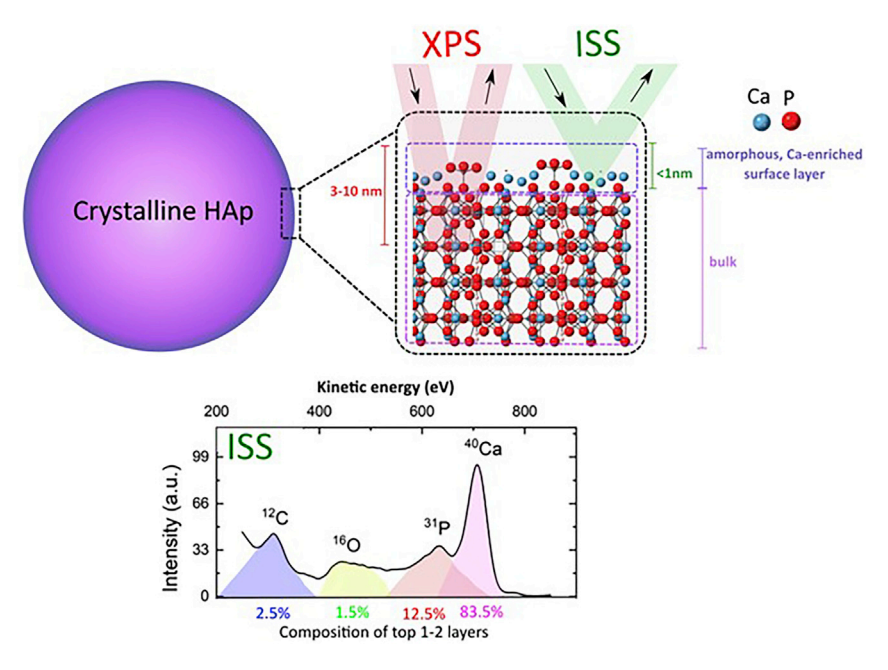


Figure 4. Surface and surface-region composition of HAp via ISS and XPS

Experimental data adapted from Uskokovic<sup>46</sup> with permission from the PCCP Owner Societies. XPS and ISS probing depths are based on Uskokovic<sup>46</sup>, Venn et al.,<sup>51</sup> Langley,<sup>52</sup> and Baltruaitis et al.<sup>53</sup>

surface. <sup>46</sup> Also, there may be an enthalpic gain if the surface OH groups and H<sub>2</sub>O form short-lived complexes via H bonding. <sup>46</sup> Another explanation for Ca enrichment of HAp at ambient conditions was postulated using the standard enthalpy of formation for Ca(OH)<sub>2</sub>, as opposed to the enthalpy of formation for protonating  $H_xPO_4^{(3-x)}$  (x=0-2) species. <sup>46</sup> The binding of OH<sup>-</sup> to Ca<sup>2+</sup> was found to be more favorable than the binding of H<sup>+</sup> to the  $H_xPO_4^{3-4}$  In agreement, another ISS (also known as low-energy ion scattering [LEIS]) study also found Ca enrichment in the topmost atomic layer in HAp. <sup>50</sup>

The Ca surface enrichment in the top atomic layer in HAp, as demonstrated by the surface-sensitive ISS, is in contrast to XPS studies, which generally point to a Ca-deficient surface, i.e., a Ca/P ratio lower than the bulk ratio across multiple literature studies. 9,11,39,46,50,54,55 The lower than bulk Ca/P ratio from XPS may be a measurement artifact, as indicated by a steady drop in the Ca/P molar ratio upon prolonged exposure to X-rays (1 h) during XPS analysis, where these ratios ranged from 0.12 to 0.30 lower than the corresponding stoichiometric values depending on the phosphate compound being studied.<sup>54</sup> It should be noted that parameters used within a study, such as the synthesis method, Ca/P ratio, identity of precursors, atmospheric composition around the synthesis vessel, etc., may also lead to contradictory results between various studies reported in the literature due to the difference in the nature of the synthesized HAp. Other than that, we believe that the compositional difference as observed by XPS (probing depth: 3-10 nm) and ISS (probing depth: top atomic layer) is justified because measurement techniques with different probing depths will give different results regarding the composition. 46,50 Therefore, a more apt interpretation of XPS results is as being a representative average of both surface and sub-surface i.e. surface region, while ISS results are representative of the true surface as shown in Figure 4. Surprisingly, near ambient pressure (NAP) XPS studies of HAp at/near reaction conditions have not been undertaken to date,



# Chem Catalysis Review

which can provide the most relevant information in contrast to ex situ XPS studies conducting measurements at ambient temperature and ultra-high vacuum (UHV) conditions. It is expected that NAP-XPS studies in conjunction with grazing incidence XRD (GIXD; also called surface XRD–SXRD) in the future will help resolve the surface composition of HAp catalysts under/near reaction conditions.

### NATURE OF HAP SURFACE SITES VIA CHEMICAL PROBE IR STUDIES

The HAp surface is known to contain acid-base pairs. <sup>19</sup> Both Lewis and Brønsted acid-base pairs may be present on the surface and, until very recently, it was not known which of these pairs are active in  $C_2H_5OH$  coupling catalysis. Specifically, a Lewis acid-base pair would be constituted of  $Ca^{2+}$  and  $OH^-$ , while a Brønsted acid-base pair of P–OH and P=O. Alternately, a *mixed* acid-base pair may also be present where a Lewis base (OH $^-$ ) is in the vicinity of a Brønsted acid (P-OH) and vice versa. The sections below are dedicated to the state-of-the-art understanding of isolated acid and base sites as well as the acid-base pairs present on HAp surfaces revealed by chemical probe IR studies.

#### Carbon monoxide (CO) IR studies

CO is well suited to obtain critical insights on the basicity and acidity of surface HAp sites.<sup>29</sup> The Lewis acid on the HAp surface was found to be weak-to-moderate in strength. Using CO adsorption IR spectroscopy, it was shown that, at 303 K, only one IR peak at 2,181 cm<sup>-1</sup> was present.<sup>56</sup> The maximum intensity of the band attained under progressively increasing CO pressures was found to be extremely low, leading to the conclusion that HAp surface cations were weak Lewis acidic sites. 56 Moreover, based on the low value of heat of adsorption calculated as a function of increasing uptake at 303 K for a HAp sample dehydrated at 573 K, it was concluded that only a small fraction ( $\sim$ 5%) of the surface Ca<sup>2+</sup> sites were acidic enough for CO adsorption, suggesting the overall weak Lewis acidity of the HAp surface. 56 Similar results of CO probing indicating weak, marginally reactive Lewis acid sites on the HAp surface were also reported. <sup>29,57,58</sup> Interestingly, one study deconvoluted the CO adsorption bands in the 2,100-2,200 cm<sup>-1</sup> range into the following five bands:  $\sim$ 2,182 cm<sup>-1</sup> from CO adsorbed on Ca<sup>2+</sup>, and the four contributions at  $\sim$ 2,177,  $\sim$ 2,171,  $\sim$ 2,164, and  $\sim$ 2,152 cm $^{-1}$  from CO interacting with various Brønsted acidic P-OH surface groups. According to this interpretation, the authors concluded that the HAp surface has both weak Lewis acidic Ca<sup>2+</sup> and Brønsted acidic P-OH sites.<sup>39</sup>

### Pyridine (C<sub>5</sub>H<sub>5</sub>N) IR spectroscopy

IR peaks at 1,597, 1,574, 1,488, and 1,441 cm $^{-1}$  observed for pyridine ( $C_5H_5N$ ) chemisorbed on HAp surface were attributed to Lewis acid sites, $^{57}$  while the peaks at 1,604, 1,588, and 1,434 cm $^{-1}$  to physisorbed pyridine. $^{57}$  As the sample was purged with He and the temperature increased, all bands decreased to almost zero by  $100^{\circ}$ C. These results confirm that pyridine weakly adsorbs on the HAp surface on Lewis acid sites—corroborating the weak strength of Lewis acid sites suggested from CO adsorption studies. Even though the authors concluded that no Brønsted acid peak was observed in 1,540–1,545 cm $^{-1}$ , a small peak (highlighted in red in Figure 5) is in fact present in the spectrum. The presence of Brønsted acidity in HAp is controversial as some reports provide evidence for their presence,  $^{55}$  while others do not. $^{29}$  The disagreement on the presence of Brønsted acid sites on the HAp surface is yet to be resolved and requires careful spectroscopic characterization of model samples prepared via various synthesis methods with different Ca/P ratios under controlled conditions of measurement. Finally, another commonly used basic probe, ammonia (NH<sub>3</sub>), could be used to verify the presence of Brønsted acid sites. It

**Review** 



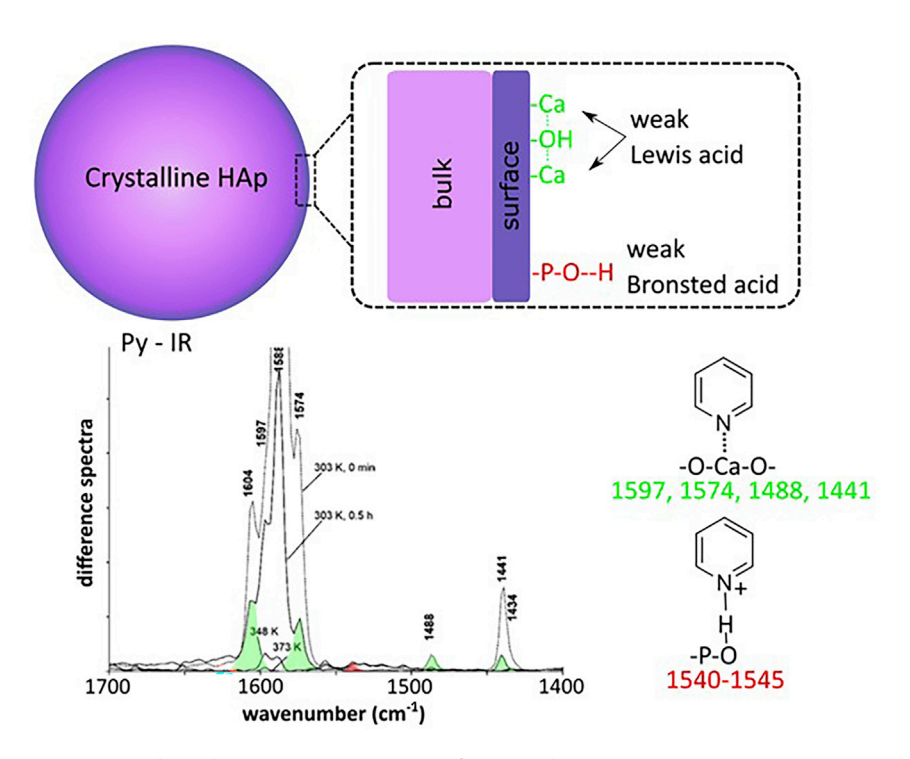


**Figure 5. Pyridine adsorption IR spectroscopy of HAp catalysts.**Weak IR peaks due to pyridine adsorption on Lewis and Brønsted acid sites were observed. . Data adapted from Hill et al., <sup>57</sup> copyright American Chemical Society.

is known that pyridine does not demonstrate Brønsted acid sites on alumina due to weak strength, <sup>59</sup> while being a much stronger base, NH<sub>3</sub> does. <sup>60</sup>

#### Carbon dioxide (CO<sub>2</sub>) IR spectroscopy

HAp naturally exhibits surface carbonates due to CO<sub>2</sub> adsorption from the environment, and bulk carbonates from dissolved  $CO_2$  in alkaline water, substituting  $PO_4^{3-}$ ions during HAp synthesis.<sup>33,38</sup> Therefore, accurately interpreting IR spectra while using CO<sub>2</sub> as a probe for surface basic sites in HAP is quite a complex task—one without a clear advantage over other more revealing probe molecules. Studies employing CO<sub>2</sub> probe IR spectroscopy for surface characterization of HAp samples have demonstrated that, upon CO2 adsorption, an increase in the pre-existing carbonates and hydroxyls in the HAp sample was observed.<sup>38</sup> To date, the exact type and structure of the adsorbed species is not fully understood, as the position and intensity of various IR peaks observed is very sensitive to the temperature of the experiment and the nature of the HAp sample. For example, as summarized in Table 1, three representative reports assign various IR peaks observed during CO<sub>2</sub> IR spectroscopy to different kinds of carbonate and bicarbonate structures in contradiction with each other. It suffices to note here that, despite disagreement in the exact band assignments—which in itself if not trivial, the formation of hydroxycarbonates/bicarbonates and other various forms of bulk and surface carbonate species upon CO<sub>2</sub> adsorption is unanimously accepted among the HAp catalysis community. 25,38,57

### Acetylene (C<sub>2</sub>H<sub>2</sub>) IR spectroscopy

Another effective probe to study the nature of surface sites in HAp is acetylene ( $C_2H_2$ ).  $C_2H_2$  can adsorb non-dissociatively onto the surface sites in various configurations: (1) a  $\pi$  complex parallel to the surface with a Brønsted or Lewis acid site via the interaction of the  $C\equiv C$  bond with the surface sites, <sup>38,57</sup> (2) a  $\sigma$  complex



Table 1. Literature summary of IR peak assignments for CO<sub>2</sub> adsorption IR studies on HAp catalysts, highlighting the disagreement on the exact type and nature of adsorbates formed

Wavenumber (cm <sup>-1</sup> )	Assignment	Reference
1,701	bicarbonate	Hill et al. <sup>57</sup>
1,624	bidentate bicarbonate	Hill et al. <sup>57</sup>
1,597	bidentate carbonate	Hill et al. <sup>57</sup>
1,360	bidentate carbonate	Hill et al. <sup>57</sup>
1,545–1,456	bulk type B carbonate	Diallo-Garcia et al. <sup>38</sup>
1,501–1,444–1,414	bulk type A carbonate	Diallo-Garcia et al. <sup>38</sup>
1,420–1,409	surface type A carbonate	Diallo-Garcia et al. <sup>38</sup>
1,485–1,385	surface (PO <sub>x</sub> ) <sub>s</sub> -carbonate	Diallo-Garcia et al. <sup>38</sup>
1,370–1,345	surface (PO <sub>x</sub> ) <sub>s</sub> -carbonate	Diallo-Garcia et al. <sup>38</sup>
1,758–1,704–1,673–1,664–1,610–1,590	$\nu$ (OCO) <sub>as</sub> bicarbonate	Diallo-Garcia et al. <sup>38</sup>
1,398 or 1,390	$\nu$ (OCO) <sub>s</sub> bicarbonate	Diallo-Garcia et al. <sup>38</sup>
1,180–1,240	δ(COH) bicarbonate	Diallo-Garcia et al. <sup>38</sup>
1,482, 1,345–1,370	monodentate carbonate on CaO-PO <sub>x</sub>	Ho et al. <sup>25</sup>
1,442–1,400	monodentate carbonate on CaO	Ho et al. <sup>25</sup>
1,710–1,590	monodentate bicarbonate	Ho et al. <sup>25</sup>
$(PO_x)_{sr}$ chemisorbed carbonates on $PO_x$ surface sites		

perpendicular to the surface with a Brønsted basic site via the interaction of one hydrogen,  $^{38}$  (3) a  $\pi\text{-}\sigma$  complex parallel to the surface with an adjacent acid-base pair.  $^{38}$  C<sub>2</sub>H<sub>2</sub> can also adsorb dissociatively onto strong basic sites, which would result in the formation of an OH group.  $^{38}$ 

The lack of perturbation in the P-O vibrations upon  $C_2H_2$  adsorption was used to conclude that the adsorption occurred at the basic OH groups and not the basic, unprotonated  $PO_4^{3-}$  sites on the surface. Results also showed that IR peaks corresponding to the P-OH groups were perturbed, suggesting that P-OH were serving as the Brønsted acid sites. No evidence for dissociative adsorption of  $C_2H_2$  on strongly basic surface sites was observed. The three unique surface sites and the three types of non-dissociative adsorptions demonstrated for acetylene on HAp are summarized below and depicted in Figure 6:

- 1. The  $\pi$  complex formation on isolated, mild Brønsted acidic sites (P-OH) led to only one C-H vibration of the acetylene molecule, with neither of the two acetylene protons being directly involved in the interaction. Therefore, the C-H vibration was only slightly red-shifted compared with the gas-phase IR peak at 3,237 cm<sup>-1</sup>. These sites are indicated in red in Figure 6.
- 2. The  $\pi$ - $\sigma$  complex formation over a Brønsted acid-base pair on the HAp surface led to two unique C-H IR peaks. The two IR peaks at 3,214 and 3,099 cm $^{-1}$  were found to be affected similarly during the desorption step and therefore assigned to a  $C_2H_2$  adsorbed non-dissociatively on an acid-base pair in a parallel configuration. Also note here that both C-H bands are red-shifted in comparison with gas-phase  $C_2H_2$ , indicating elongation. These sites are indicated in green in Figure 6.
- 3. The  $\sigma$  complex formation on isolated, medium-strength Brønsted basic sites (OH) led to two distinct C-H bands at 3,178 and 3,281 cm $^{-1}$ . In this case, one C-H bond is elongated due to interaction with a basic surface OH site, while the other hydrogen of  $C_2H_2$ , which is at the other end and dangling, is shortened compared with gas-phase  $C_2H_2$ , indicating perpendicular adsorption of  $C_2H_2$  onto a surface hydroxyl. These species are indicated in blue in Figure 6.

Review



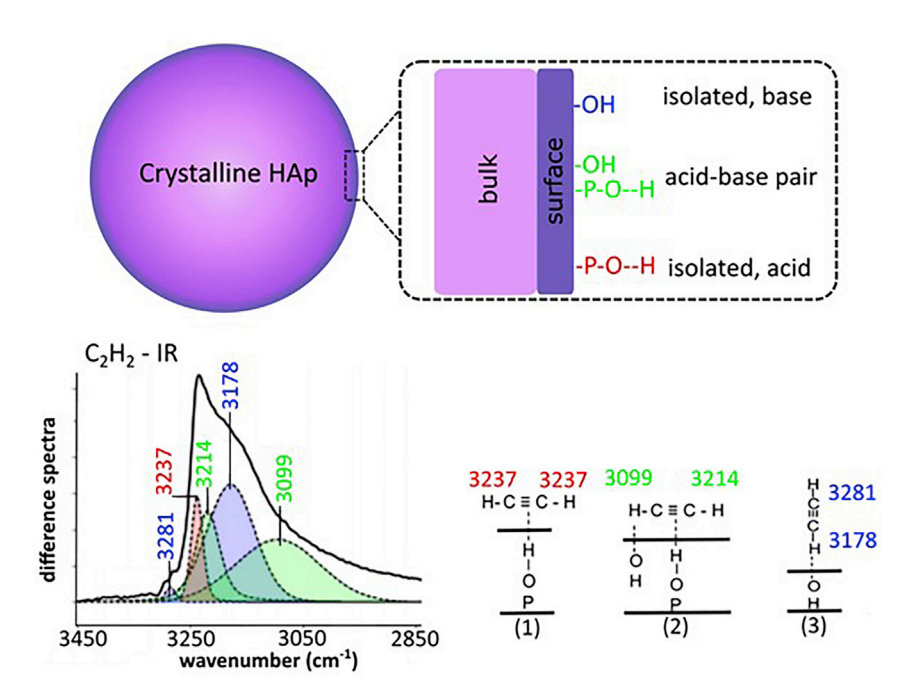


Figure 6. Acetylene adsorption IR spectroscopy of HAp catalysts.

Surface acidic and basic sites probed with  $C_2H_2$  adsorption suggest the presence of Brønsted acid sites (P-OH) and Brønsted base sites (-OH) on the surface.

Data adapted from Diallo-Garcia et al., 38 copyright American Chemical Society.

Summarily, C<sub>2</sub>H<sub>2</sub> adsorbed non-dissociatively onto the HAp surface and predominantly interacted with the surface OH groups. These weakly basic OH groups (presumably Ca-OH) were involved in two non-dissociative adsorption modes. As the PO<sub>4</sub><sup>3-</sup> IR peaks were not perturbed by C<sub>2</sub>H<sub>2</sub> adsorption, it was concluded that the basic  $O^{2-}$  of  $PO_4^{3-}$  is not involved in  $C_2H_2$  adsorption or might not be present on the surface. The absence of P-O perturbation upon C<sub>2</sub>H<sub>2</sub> adsorption also corroborates findings from the MAS-NMR study, which suggested that the HAp surface, even at elevated temperature, is largely populated with H<sub>x</sub>PO<sub>4</sub><sup>(3-x)</sup> and not with PO<sub>4</sub><sup>3-.36</sup> Note, that when the OH groups are associated with P, as in P-OH, they become mild-strength Brønsted acid sites. Since these mildly acidic P-OH sites were found to be involved in a non-dissociative C<sub>2</sub>H<sub>2</sub> adsorption mode, their role in catalytic reactions becomes relevant. Most importantly, the presence of acidbase pairs on the HAp surface that led to  $\pi$ - $\sigma$  complex formation upon  $C_2H_2$  adsorption is a unique site that requires further attention and evaluation, given their critical relevance to acid-base (bifunctional) catalytic applications. Avenues requiring further work include (1) quantifying the density of such acid-base pairs on HAp surfaces with relevance to Ca/P ratio and various synthesis techniques, (2) understanding and tuning the strength of isolated acid or base sites versus the acid-base pairs, and (3) unraveling the role of acid-base pairs and isolated sites in catalytic reactions via operando and modulation-excitation characterization techniques.

# RATIONALIZING STRUCTURE-REACTIVITY RELATIONSHIPS IN HAP-CATALYZED C=C COUPLING

C–C coupling of alcohols constitutes a large volume of reports on HAp catalysis, and the following discussion will focus on the structure-function relationships of HAp catalysts during C–C coupling reactions. Rigorous evidence (spectroscopy; transient kinetics; steady-state kinetics) in the literature point toward ethanol to butanol

Review

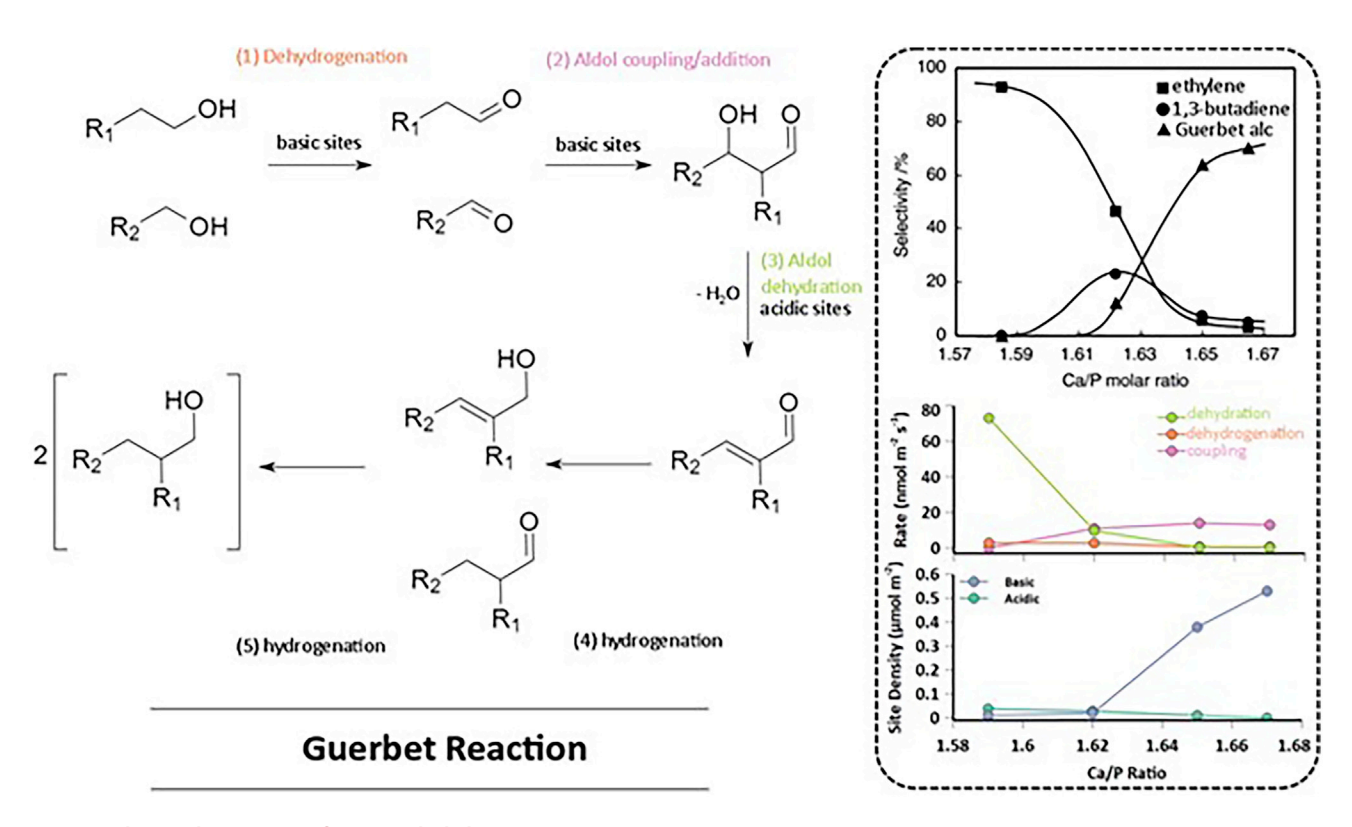


Figure 7. The Guerbet reaction of primary alcohols

(Left) Guerbet reaction mechanism for primary alcohols. (Right) Panels showing the dependence of reaction rates and product selectivities in Guerbet coupling of ethanol on the acidic and basic nature of surface sites in HAp. As the Ca/P molar ratio increases, the density of basic sites also increases, resulting in a systematic decrease in the acid-catalyzed dehydration step rate. Likewise, as the Ca/P increases, the surface basic site density also increases and, as a result, the selectivity to ethylene by-product (from acid-catalyzed dehydration of ethanol) decreases while the selectivity toward Guerbet-coupled alcohols (desired) increases, indicating the importance of basic surface site density for the Guerbet mechanism. Finally, selectivity toward 1,3-butadiene by-product formation from dehydration of crotonaldehyde intermediate goes through a maximum value because, at Ca/P of ~1.62, an optimum balance is reached between the acidic and basic surface site densities, which was hypothesized to promote a secondary reaction pathway "Lebedev reaction" where 1,3-butadiene is the main product. Information and figure are adapted from Tsuchida et al. 11 and Kozlowski and Davis. 17

reaction following the Guerbet mechanism. 17-19,22,24,25,28,61 However, some evidence is present in the literature from 2014–2015 for the so-called 'direct' mechanism of ethanol coupling as well. <sup>20,62</sup> Given the general consensus on the Guerbet mechanism, we will discuss the surface chemistry of HAp with regard to Guerbet mechanism only. Utilizing HAp for n-C<sub>4</sub>H<sub>9</sub>OH synthesis via the Guerbet reaction of C<sub>2</sub>H<sub>5</sub>OH circumvents the previously employed industrial Oxo process.<sup>63</sup> The Oxo process consists of two successive reactions: the hydroformylation of propylene with syngas (carbon monoxide and hydrogen) from crude oil over cobalt or rhodium catalysts at high pressure to synthesize aldehyde, and the hydrogenation of this aldehyde over a nickel catalyst to yield  $n-C_4H_9OH$ . The Oxo process is extremely problematic from both economical and environmental standpoints, as it requires a high-pressure reaction of propylene with syngas—a steam reforming product. A pioneering study from 2006, 63 reported Hap-catalyzed coupling of C<sub>2</sub>H<sub>5</sub>OH into n-C<sub>4</sub>H<sub>9</sub>OH with a 76% selectivity at atmospheric pressure, which initiated the vibrant field of catalytic upgrading of bio-feedstock relevant alcohols (especially C<sub>2</sub>H<sub>5</sub>OH) into higher-value fuels and chemicals.

The general Guerbet reaction mechanism, depicted in Figure 7, encompasses the most widely accepted five reaction steps that were verified by kinetic isotope switch

**Review** 



experiments and spectroscopy. The first step of the catalytic Guerbet reaction involves oxidation (dehydrogenation) of the primary alcohol over the basic sites to form corresponding surface-bound aldehyde species, which undergo aldol condensation over basic surface sites to yield the surface-bound condensation product. This condensation product then dehydrates to unsaturated aldehyde surface-bound species over the acidic surface sites of the catalyst. Once the unsaturated aldehyde species are formed, they undergo hydrogenation either on the surface or in the gas phase to produce the final product. To highlight the importance of acid-base sites for the corresponding steps involved in the Guerbet reaction, the right panel in Figure 7 shows the variation in Ca/P ratio, which likely changes the surface acid-base site balance and consequently the selectivity of the HAp-based catalysts by controlling the rate of dehydration, dehydrogenation, and aldol-coupling steps. 21 Contrary to previous assumptions, a study has also shown that the Ca/P ratio does not always correlate directly with the acidity or basicity of the HAp catalysts. Specifically, the Ca/P = 1.65 sample was shown to be more basic (and hence more active for the oxidation of a probe molecule 2-methyl-3-butyn-2-ol) than samples with Ca/P = 1.67 and 1.77. 10 The Ca/P ratio was confirmed using inductively coupled plasma atomic emission spectroscopy, and the authors hypothesized that, besides the Ca/P ratio, the degree of carbonation and the amount of OH defects in HAp also contribute toward the final acidic and basic character of the surface sites. 10 Given the dependence of reaction rates for each step on surface acid-base sites, the importance of state-of-the-art understanding regarding the composition of a surface, the nature of those acid and base sites provided in the previous sections becomes clear.

#### C<sub>2</sub>H<sub>5</sub>OH interaction with the surface sites; steps 1–3

The HAp surface is populated by weak acidic and moderate strength basic sites, which also exist as acid-base pairs.  $C_2H_5OH$  adsorption on HAp surface sites constitutes the first elementary step in Guerbet-type reactions. An important distinction is regarding the identity of adsorption sites and the mode of adsorption.  $C_2H_5OH$  can adsorb on the surface in two ways, e.g., (1) molecularly as intact  $C_2H_5OH^*$  and (2) dissociatively as  $C_2H_5O^*$  and  $H^*.^{64-66}$  For molecularly adsorbed species, the final structure of the adsorbate resembles that of the free  $C_2H_5OH$  molecule. On the other hand, the dissociatively adsorbed species lead to surface bound species, such as  $C_2H_5O^*$ , and indicate more favorable (exothermic) binding to the surface sites.

Upon C<sub>2</sub>H<sub>5</sub>OH adsorption at room temperature on HAp, three distinct bands were observed in the C-H region: 2,975  $v_{as}(CH_3)$ , 2,930  $v_{as}(CH_2)$ , and 2,903 cm<sup>-1</sup>  $v_{as}(CH_3)$ , corresponding to the ethoxy species formed from dissociatively adsorbed  $C_2H_5OH.^{61,67}$  Given the decrease in intensity of  $\sim 3,570$  and  $\sim 3,670$  cm<sup>-1</sup> peaks upon C<sub>2</sub>H<sub>5</sub>OH adsorption, it was concluded that adsorption occurred on both Lewis basic OH<sup>-</sup> and Brønsted acidic P-OH sites. <sup>67</sup> Elsewhere in the literature, adsorption of propanal (C<sub>3</sub>H<sub>6</sub>O) on surface Lewis basic (OH<sup>-</sup>) and Brønsted acid (P-OH) sites on HAp also supports the involvement of these sites in adsorption. <sup>29</sup> However, the literature does not discuss the effect of  $C_2H_5OH$  adsorption on the  $\sim$ 3,500 cm<sup>-1</sup> band that is observed but not assigned across various reports, as highlighted in a previous section of this review. Moreover, while a decrease in IR peak intensities suggests interaction between adsorption sites and the adsorbate, TPD-IR studies are absent that can shed light if any new O-H sites are generated in situ as the adsorbed C<sub>2</sub>H<sub>5</sub>OH desorbs/reacts with increasing temperature. Two new peaks were observed upon C<sub>2</sub>H<sub>5</sub>OH adsorption at 1,385 and 1,495 cm<sup>-1</sup>, which were attributed to adsorbed ethoxy ( $C_2H_5O^*$ ) and acetate (CH<sub>3</sub>COO\*) species on the HAp surface, respectively. <sup>67</sup> A weak shoulder at 1,660 cm<sup>-1</sup> further corroborated the presence of C-O vibrations from surface acetate species. As the temperature increased, IR bands



# Chem Catalysis Review

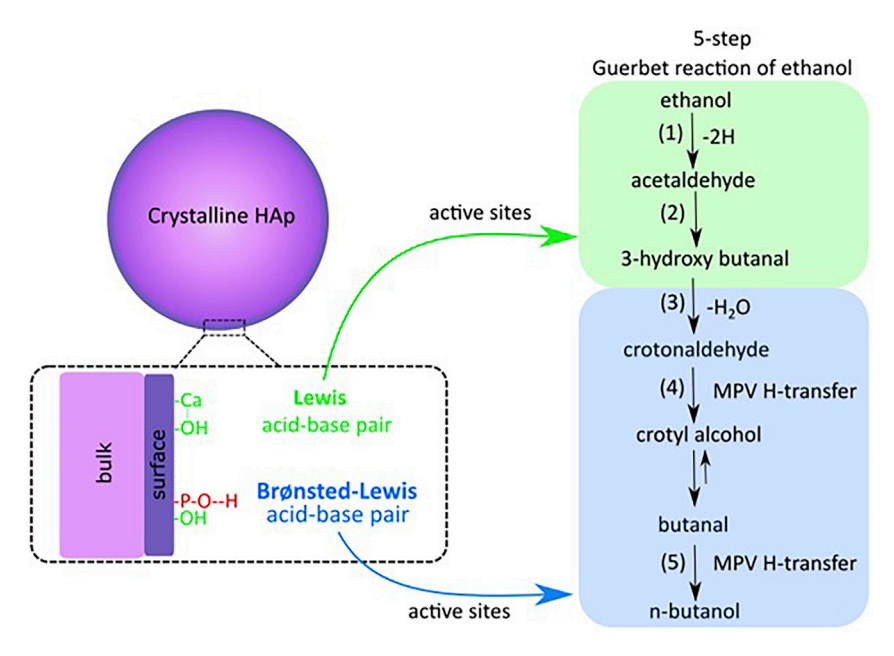


Figure 8. Summary of literature proposed active sites for various steps in the Guerbet reaction of  $C_2H_5OH$  to n- $C_4H_9OH$  over HAp catalysts

corresponding to ethoxy species weakened significantly, and completely disappeared by 573 K, indicating the moderate strength of adsorption sites. 61 Surprisingly, no vibration in the carbonyl region (1,700–1,800 cm<sup>-1</sup>) was reported upon C<sub>2</sub>H<sub>5</sub>OH adsorption on HAp in any IR spectroscopy study<sup>19</sup> until recently, where a modulation-excitation approach demonstrated an IR peak at 1,758 cm<sup>-1</sup>, confirming the formation of surface-bound acetaldehyde (CH<sub>3</sub>CHO). <sup>19</sup> We caution the reader that a majority of studies reporting in situ IR spectroscopy of C<sub>2</sub>H<sub>5</sub>OH-adsorption on HAp do so at low temperatures where condensed phase ethanol may be present, and do not employ the informative TPD approach. Conducting IR studies with flowing C<sub>2</sub>H<sub>5</sub>OH throughout the duration of the study is also problematic, as water and condensed  $C_2H_5OH$  can be present on the surface at low temperatures ( $\sim$ 373 K), obscuring the weaker intensity bands and their respective assignments from the reaction intermediates. To the best of our knowledge, a systematic TPD-IR study has also not been conducted on the strength and density of C<sub>2</sub>H<sub>5</sub>OH binding sites in HAp as a function of Ca/P ratio to unravel the effect of surface acid-base balance on interaction with probe or reactant molecules. Therefore, TPD-IR studies are necessary to further understand HAp catalysts under working conditions.

It is generally accepted that surface-bound ethoxy is dehydrogenated/oxidized to acetaldehyde, which self-aldol couples over basic sites.  $^{19,21}$  The coupling product then likely dehydrates over Brønsted acidic sites to yield crotonaldehyde, completing the aldol condensation pathway.  $^{19,21}$  Although there was uncertainty regarding the active sites for the Guerbet reaction over HAp, as summarized in Figure 8 based on recent modulation-excitation (M-E)-DRIFTS results, it is likely that the Lewis acid-base pair ( $\rm Ca^{2+}$  and  $\rm OH^-$ ) serves as the active sites for steps 1–2 of the Hap-catalyzed Guerbet reaction to produce  $\it n-C_4H_9OH$  from  $\rm C_2H_5OH$ .  $^{19}$  Elsewhere, poisoning experiments with two acidic probe molecules of different acidic strengths, i.e.,  $\rm CO_2$  and propionic acid revealed that acetaldehyde and butanol formation rates decreased to varying extents with the introduction of each acidic probe, demonstrating that the basic sites for the various reaction steps, specifically step 1 versus

**Review** 



steps 2–5, are not identical. <sup>25</sup> Based on complementary *in situ*  $CO_2$  IR study results, it was further suggested that ethanol dehydrogenation to acetaldehyde was likely catalyzed by the Ca-O surface sites where the  $CO_2$  probe adsorbed weakly, leading to a lack of significant inhibitory effect. On the other hand, all subsequent steps to yield the butanol product were proposed to be over Ca-O-PO<sub>x</sub> interfacial sites, where acidic probes, such as  $CO_2$ , adsorbed strongly and exhibited a severe inhibitory effect. <sup>25</sup>

Critical insights inferred from kinetics studies also corroborate the spectroscopic insights summarized above. For example, the steady-state rate of aldol condensation of acetaldehyde to crotonaldehyde (steps 2-3) over HAp showed an approximately first-order dependence on acetaldehyde partial pressure, and an extremely low activation barrier as the reaction was found to be temperature independent.<sup>28</sup> Moreover, isotope switch experiments using fully deuterated acetaldehyde did not exhibit a kinetic isotope effect in the first-order rate constant in comparison with the H-form acetaldehyde, suggesting that C-H activation was not kinetically relevant and likely not involved in the rate-determining step. <sup>28</sup> These results signified that the C-H activation cannot be the kinetically relevant reaction step and hence enolate formation (i.e., α-H abstraction from the surface-bound aldehyde) was not the slow step. Other aldol condensation steps do not involve C-H activation and thus can be ruled out as rate determining.<sup>28</sup> It was suggested that the rate-determining steps likely were the desorption of products, including crotonaldehyde and water.<sup>28</sup> A recent in-depth kinetic study confirmed that competitive adsorption of water inhibits ethanol coupling over HAp; however, this inhibition can be fully reversed by removing water from the feed.<sup>24</sup> It should be noted that the C-H activation is not kinetically relevant if acetaldehyde aldol condensation to crotonaldehyde is being studied exclusively. However, if the full Guerbet reaction of ethanol to n-butanol over HAp is considered where acetaldehyde intermediate is formed from ethanol dehydrogenation,<sup>25</sup> followed by acetaldehyde aldol condensation to crotonaldehyde, and finally hydrogenation of crotonaldehyde to n-butanol, the C-H activation step during aldol coupling does become kinetically relevant. 24,25,61 As the Guerbet reaction involves hydrogenation of surface-bound aldol condensation intermediates, the product desorption barrier likely decreases due to hydrogenation, making desorption facile.

### Hydrogenation during the Guerbet reaction of C<sub>2</sub>H<sub>5</sub>OH; steps 4–5

The hydrogenation steps (4–5) in the Hap-catalyzed Guerbet reaction were not well understood until recently. Two different hydrogenation pathways can be possible: (1) surface-mediated hydrogenation of the C=C bond of unsaturated alcohol (crotyl alcohol), where the surface hydrogen comes from C<sub>2</sub>H<sub>5</sub>OH dehydrogenation in the first step, 19,68,69 and (2) direct hydrogenation of C=O in butanal (from isomerization + tautomerization of crotyl alcohol) by C<sub>2</sub>H<sub>5</sub>OH via the Meerwein-Ponndorf-Verley (MPV) reaction. 18,19,27,68 On transition metal catalysts, such as copper, gas-phase molecular hydrogen rapidly exchanges, <sup>17</sup> so the hydrogenation and dehydrogenation mechanisms on metal-containing catalysts are usually surface mediated. However, hydrogenation/dehydrogenation mechanisms on metal oxides and metal phosphates are not well understood and expected to be different than their metal counterparts. 17 Recent literature has provided more evidence of MPV mechanism prevailing over HAp as D<sub>2</sub> and H<sub>2</sub> isotopic exchange did not occur over HAp, and, upon D<sub>2</sub> introduction, deuterated products were not observed, indicating that hydrogen for the hydrogenation reaction steps was sourced from the reactant C<sub>2</sub>H<sub>5</sub>OH molecules. <sup>18,19</sup> Moreover, all of the hydrogen transfer reactions (i.e., steps 4-5) during Guerbet coupling involve MPV-like Please cite this article in press as: Kiani and Baltrusaitis, Surface chemistry of hydroxyapatite for sustainable *n*-butanol production from bio-ethanol, Chem Catalysis (2021), https://doi.org/10.1016/j.checat.2021.06.005



# Chem Catalysis Review

reactions between the sacrificial H-donor alcohol and the C=O intermediates.  $^{18}$  No evidence for C=C hydrogenation was observed, which suggests hydrogenation via MPV-hydrogen transfer steps likely undergo a double bond shift to form an enol, which is tautomerized to a C=O before hydrogenation.  $^{18}$  In agreement with these findings, recent *operando* M-E-DRIFTS also provide spectroscopic evidence for hydrogenation of C=O in butanal intermediate.  $^{19}$  The M-E-DRIFTS results point toward a hydrogen transfer between reactant  $C_2H_5OH$  and intermediate butanal to form n- $C_4H_9OH$  product over P-OH – OH $^-$  acid-base pair on the HAp surface.  $^{19}$  The relevance of the MPV hydrogenation pathway to surface P-OH sites was also corroborated by the fact that, when Brønsted acidic P-OH sites are selectively poisoned, the n- $C_4H_9OH$  product from hydrogenation of butanal intermediate is not observed.  $^{32}$ 

Summarily, based on the literature analyzed within this review, the Lewis acid-base pair (Ca<sup>2+</sup>–OH<sup>-</sup>) is proposed to be the main active site for steps 1–2 of the Guerbet reaction, which includes dehydrogenation and aldol coupling. On the other hand, the Brønsted-Lewis acid-base pair (P-OH–OH<sup>-</sup>) is proposed as the main site for steps 3–5, including dehydration of the aldol coupling product to complete aldol condensation, and subsequent hydrogenation of unsaturated aldol products (C=O) via the MPV route. Note that this distinctive Brønsted-Lewis acid-base pair was first identified as a surface site unique to HAp via acetylene IR spectroscopy.<sup>38</sup> Noting the linear length of the acetylene molecule, <sup>70,71</sup> it is suggested that this acid-base pair is ca. 166 pm (1.6 Å) apart. The proposed active sites are summarized in Figure 8.

### **OUTLOOK**

Overall, the HAp catalysis literature seems to suggest that the Lewis acid-base pair (Ca<sup>2+</sup>-OH<sup>-</sup>) is the main active site for steps 1-2 of the Guerbet reaction, which includes dehydrogenation and aldol coupling, while Brønsted-Lewis acid-base pair (P-OH-OH<sup>-</sup>) seems to be the main active site for steps 3-5, including dehydration of the aldol coupling product to complete aldol condensation, and subsequent hydrogenation of unsaturated aldol products via the MPV route. However, a few critical pieces of the surface mechanism remain unclear. Previously, it has been proposed that the primary handle on HAp acid and basic properties was the Ca/P molar ratio, adjusted by varying the precursor concentrations during synthesis. However, recent studies employing advanced characterization of HAp samples demonstrate that the surface chemistry is much more complex. 17-19,21 By using test reactions in conjunction with detailed surface characterization, it has been shown that, even at a stoichiometric Ca/P ratio of 1.67, the degree of carbonation during synthesis and the population of OH and related defects strongly affect the bifunctional (acid-base) nature of the final HAp catalyst. Another reason for the discrepancy between the hypothesized activity of various acid-base sites toward each reaction step in C-C coupling and the observed rates can be the use of unsuitable probe molecules utilized in spectroscopic studies. Experts in the field acknowledge that more reactant-like probe molecules are needed to be used to effectively probe the nature of surface sites in HAp and generate reaction-relevant mechanistic insights. 17

It is proposed that further advancement of the fundamental structure-reactivity relationships of Hap-catalyzed C–C coupling reactions that can address the information gap and guide the rational design of improved catalysts will require the following:

Review



- 1. In situ and operando temperature-programmed spectroscopic studies, especially IR and Raman spectroscopy, and NAP-XPS of HAp-catalyzed C-C coupling reactions to elucidate the structural and compositional dynamics of various surface species being generated or consumed at/near reaction conditions. The most advanced studies will also involve modulation-excitation spectroscopy, as recently demonstrated. 19 During modulation-excitation, when a catalytic system is perturbed via modulation of a parameter (e.g., reactant partial pressure) under quasi-steady-state conditions, reaction intermediates will oscillate with the same frequency as the perturbation. After multiple data are averaged during modulation-excitation, the signal from active surface species will be enhanced while the spectator surface species will not respond to the stimulation, providing researchers an unprecedented tool to distinguish spectator surface species. 19,72 Finally, ISS (also called LEIS) and GIXD/SXRD<sup>73-75</sup> studies need to be conducted on a series of well-defined HAp catalysts to ascertain the true surface composition of catalysts (i.e., surface termination/enrichment) and its effect on the C<sub>2</sub>H<sub>5</sub>OH coupling activity and selectivity of those catalysts.
- 2. It is known that moderately basic and weakly acidic sites are required for an effective Guerbet reaction catalyst, which HAp surface is known to possess. Future studies need to characterize and test model catalysts to shed light on the proximity of the acid-base pair, and what makes those sites unique to HAp. It is yet to be ascertained whether a monolayer catalyst with H<sub>x</sub>PO<sub>y</sub> and CaO<sub>x</sub> surface sites supported on a high surface area support can replace the traditionally used low surface area HAp catalysts. Moreover, the role of surface P=O sites in HAp toward the Guerbet reaction has not been studied in detail. For example, recently spectroscopic evidence has emerged for the involvement of such P=O surface sites participating in surface-mediated H transfer reaction, where ethanol serves as the H-donor.<sup>23</sup> Therefore, the role of P=O surface sites and their potential involvement in the surface-mediated H transfer reaction (i.e., steps 4–5 of the Guerbet reaction) needs to be studied further.
- 3. Since the structure and nature of PO<sub>x</sub> and H<sub>x</sub>PO<sub>y</sub> in the topmost atomic layer of HAp is not well known (isolated PO<sub>x</sub> versus dimeric versus oligomeric; isolated H<sub>x</sub>PO<sub>y</sub> versus dimeric versus oligomer), model catalysts need to be studied with phosphates supported on high surface area supports as a function of Ca promotion and P loading to elucidate the nature and structure of surface H<sub>x</sub>P<sub>y</sub>O<sub>z</sub>. In situ and operando Raman spectroscopy can be utilized to systematically distinguish between various types of surface H<sub>x</sub>P<sub>y</sub>O<sub>z</sub> sites. Reactivity for such model catalysts can be explicitly studied via transient methods, including temperature-programmed surface reaction.<sup>76</sup>
- 4. Elsewhere in the literature, it is known that HAp possesses OH<sup>-</sup> ion channels ~3 Å in diameter, which enable the mobility of OH ions in the bulk. Likewise, another study has also reported sinusoidal H<sup>+</sup> channels within HAp, with proton mobility demonstrated at 298–923 K. To date, a profound mechanistic role of these OH<sup>-</sup> and H<sup>+</sup> channels in HAp-catalyzed reactions (especially ethanol coupling) has not been elucidated. While most HAp catalysis literature does not allude to these channels otherwise discussed in bio-related applications of HAp, some recent reports have started to appreciate and investigate their role toward C-H activation over HAp-based catalysts. Dedicated computational and experimental studies are required to fully ascertain the potential role of these channels unique to HAp toward catalytic applications. Curious readers are directed to mechanistic studies from broader literature regarding the unique ion channels and how they affect HAp's properties. To have the base of the ba



5. Finally, the potential involvement of acidic  $H_xCO_3^{(2-x)}$  surface sites needs to be studied with respect to various reaction steps in the Guerbet mechanism using *in situ* and *operando* spectroscopic studies including chemical probe IR spectroscopy. For instance, the H-transfer capability of carbonate surface sites has been demonstrated: it was observed thatin the absence of water, carbonic acid ( $H_2CO_3$ ) surface intermediate formed upon adsorption of various H-donor probe molecules ( $CH_3COOH$ ,  $HNO_3$ , HCOOH) onto  $CaCO_3$  where surface  $H_xCO_3^{(2-x)}$  sites were present and transfered the hydrogen from the H-donor molecules. <sup>84</sup> Therefore, a systematic study is required to elucidate how the surface chemistry of HAp catalysts is influenced by surface  $H_xCO_3^{(2-x)}$  sites by using model catalytic systems and suitable probe molecules.

#### **ACKNOWLEDGMENTS**

This work is supported by NSF CBET 1706581. D.K. acknowledges the John C. Chen endowed Fellowship for financial support.

#### **DECLARATION OF INTERESTS**

The authors declare no competing interests.

### **REFERENCES**

- Grim, R.G., To, A.T., Farberow, C.A., Hensley, J.E., Ruddy, D.A., and Schaidle, J.A. (2019). Growing the bioeconomy through catalysis: a review of recent advancements in the production of fuels and chemicals from syngasderived oxygenates. ACS Catal. 9, 4145–4172.
- Abdulrazzaq, H.T., and Schwartz, T.J. (2019). Chapter 1. Catalytic conversion of ethanol to commodity and specialty chemicals. In Ethanol, A. Basile, A. Iulianelli, F. Dalena, and T.N. Veziroğlu, eds. (Elsevier), pp. 3–24.
- Michaels, W., Zhang, H., Luyben, W.L., and Baltrusaitis, J. (2018). Design of a separation section in an ethanol-to-butanol process. Biomass Bioenergy 109, 231–238.
- Andersen, V.F., Anderson, J.E., Wallington, T.J., Mueller, S.A., and Nielsen, O.J. (2010). Vapor pressures of alcohol—gasoline blends. Energy Fuels 24, 3647–3654.
- Bruno, T.J., Wolk, A., and Naydich, A. (2009). Composition-explicit distillation curves for mixtures of gasoline with four-carbon alcohols (butanols). Energy Fuels 23, 2295–2306.
- US Department of Energy Office of Energy Efficiency & Renewable Energy. Biobutanol. https://afdc.energy.gov/fuels/emerging\_ biobutanol.html.
- Usami, K., Xiao, K., and Okamoto, A. (2019). Efficient ketose production by a hydroxyapatite catalyst in a continuous flow module. ACS Sustain. Chem. Eng. 7, 3372– 3377.
- Uskokovic, V. (2015). The role of hydroxyl channel in defining selected physicochemical peculiarities exhibited by hydroxyapatite. RSC Adv. 5, 36614–36633.
- Rodrigues, E.G., Keller, T.C., Mitchell, S., and Pérez-Ramírez, J. (2014). Hydroxyapatite, an exceptional catalyst for the gas-phase deoxygenation of bio-oil by aldol condensation. Green. Chem. 16, 4870–4874.

- Ben Osman, M., Krafft, J.M., Millot, Y., Averseng, F., Yoshioka, T., Kubo, J., and Costentin, G. (2016). Molecular understanding of the bulk composition of crystalline nonstoichiometric hydroxyapatites: application to the rationalization of structure– reactivity relationships. Eur. J. Inorg. Chem. 2016. 2709–2720.
- Tsuchida, T., Kubo, J., Yoshioka, T., Sakuma, S., Takeguchi, T., and Ueda, W. (2008). Reaction of ethanol over hydroxyapatite affected by Ca/P ratio of catalyst. J. Catal. 259, 183–189.
- Bett, J.A.S., Christner, L.G., and Hall, W.K. (1967). Hydrogen held by solids. XII. Hydroxyapatite catalysts. J. Am. Chem. Soc. 89, 5535–5541.
- Diallo-Garcia, S., Laurencin, D., Krafft, J.-M., Casale, S., Smith, M.E., Lauron-Pernot, H., and Costentin, G. (2011). Influence of magnesium substitution on the basic properties of hydroxyapatites. J. Phys. Chem. C 115, 24317– 24327.
- 14. Elliott, J.C. (1971). Monoclinic space group of hydroxyapatite. Nat. Phys. Sci. 230, 72.
- Uysal, I., Severcan, F., Tezcaner, A., and Evis, Z. (2014). Co-doping of hydroxyapatite with zinc and fluoride improves mechanical and biological properties of hydroxyapatite. Prog. Nat. Sci. Mater. Int. 24, 340–349.
- Kay, M.I., Young, R.A., and Posner, A.S. (1964). Crystal structure of hydroxyapatite. Nature 204, 1050–1052.
- Kozlowski, J.T., and Davis, R.J. (2013). Heterogeneous catalysts for the Guerbet coupling of alcohols. ACS Catal. 3, 1588–1600.
- Young, Z.D., and Davis, R.J. (2018). Hydrogen transfer reactions relevant to Guerbet coupling of alcohols over hydroxyapatite and magnesium oxide catalysts. Catal. Sci. Technol. 8, 1722–1729.

- Wang, S.-C., Cendejas, M.C., and Hermans, I. (2020). Insights into ethanol coupling over hydroxyapatite using modulation excitation operando infrared spectroscopy. ChemCatChem 12, 4167—4175.
- Chieregato, A., Velasquez Ochoa, J., Bandinelli, C., Fornasari, G., Cavani, F., and Mella, M. (2015). On the chemistry of ethanol on basic oxides: revising mechanisms and intermediates in the Lebedev and Guerbet reactions. ChemSusChem 8, 377–388.
- Silvester, L., Lamonier, J.-F., Faye, J., Capron, M., Vannier, R.-N., Lamonier, C., Dubois, J.-L., Couturier, J.-L., Calais, C., and Dumeignil, F. (2015). Reactivity of ethanol over hydroxyapatite-based Ca-enriched catalysts with various carbonate contents. Catal. Sci. Technol. 5, 2994–3006.
- 22. Gabriëls, D., Hernández, W.Y., Sels, B., Van Der Voort, P., and Verberckmoes, A. (2015). Review of catalytic systems and thermodynamics for the Guerbet condensation reaction and challenges for biomass valorization. Catal. Sci. Technol. 5, 3876–3902.
- Kiani, D., and Baltrusaitis, J. (2021). A spectroscopic study of supported-phosphatecatalysts (SPCs): evidence of surface-mediated hydrogen-transfer. ChemCatChem. https:// doi.org/10.1002/cctc.202001897.
- Eagan, N.M., Lanci, M.P., and Huber, G.W. (2020). Kinetic modeling of alcohol oligomerization over calcium hydroxyapatite. ACS Catal. 10, 2978–2989.
- Ho, C.R., Shylesh, S., and Bell, A.T. (2016). Mechanism and kinetics of ethanol coupling to butanol over hydroxyapatite. ACS Catal. 6, 939–948.
- Zahouily, M., Abrouki, Y., Bahlaouan, B., Rayadh, A., and Sebti, S. (2003).
   Hydroxyapatite: new efficient catalyst for the Michael addition. Catal. Commun. 4, 521–524.

### **Review**

**CellPress** 

- Ogo, S., Onda, A., Iwasa, Y., Hara, K., Fukuoka, A., and Yanagisawa, K. (2012). 1-Butanol synthesis from ethanol over strontium phosphate hydroxyapatite catalysts with various Sr/P ratios. J. Catal. 296, 24–30.
- Young, Z.D., Hanspal, S., and Davis, R.J. (2016). Aldol condensation of acetaldehyde over titania, hydroxyapatite, and magnesia. ACS Catal. 6, 3193–3202.
- Hernández-Giménez, A.M., Ruiz-Martínez, J., Puértolas, B., Pérez-Ramírez, J., Bruijnincx, P.C.A., and Weckhuysen, B.M. (2017).
   Operando spectroscopy of the gas-phase aldol condensation of propanal over solid base catalysts. Top. Catal. 60, 1522–1536.
- Fihri, A., Len, C., Varma, R.S., and Solhy, A. (2017). Hydroxyapatite: a review of syntheses, structure and applications in heterogeneous catalysis. Coord. Chem. Rev. 347, 48–76.
- Haider, A., Haider, S., Han, S.S., and Kang, I.-K. (2017). Recent advances in the synthesis, functionalization and biomedical applications of hydroxyapatite: a review. RSC Adv. 7, 7442– 7458
- Osman, M.B., Krafft, J.M., Thomas, C., Yoshioka, T., Kubo, J., and Costentin, G. (2019). Importance of the nature of the active acid/ base pairs of hydroxyapatite involved in the catalytic transformation of ethanol to n-butanol revealed by OperandoDRIFTS. ChemCatChem 11, 1765–1778.
- Hua Cheng, Z., Yasukawa, A., Kandori, K., and Ishikawa, T. (1998). FTIR study on incorporation of CO<sub>2</sub> into calcium hydroxyapatite. J. Chem. Soc. Faraday Trans. 94, 1501–1505.
- 34. Elliot, J.C. (1994). Structure and Chemistry of the Apatites and Other Calcium Orthophosphates (Elsevier).
- Laurencin, D., Wong, A., Dupree, R., and Smith, M.E. (2008). Natural abundance <sup>43</sup>Ca solidstate NMR characterisation of hydroxyapatite: identification of the two calcium sites. Magn. Reson. Chem. 46, 347–350.
- Ben Osman, M., Diallo-Garcia, S., Herledan, V., Brouri, D., Yoshioka, T., Kubo, J., Millot, Y., and Costentin, G. (2015). Discrimination of surface and bulk structure of crystalline hydroxyapatite nanoparticles by NMR. J. Phys. Chem. C 119, 23008–23020.
- Panda, R.N., Hsieh, M.F., Chung, R.J., Chin, T.S., and FTIR, X.R.D. (2003). SEM and solid state NMR investigations of carbonatecontaining hydroxyapatite nano-particles synthesized by hydroxide-gel technique. J. Phys. Chem. Sol. 64, 193–199.
- Diallo-Garcia, S., Osman, M.B., Krafft, J.-M., Casale, S., Thomas, C., Kubo, J., and Costentin, G. (2014). Identification of surface basic sites and acid-base pairs of hydroxyapatite. J. Phys. Chem. C 118, 12744–12757.
- Ben Osman, M., Diallo Garcia, S., Krafft, J.-M., Methivier, C., Blanchard, J., Yoshioka, T., Kubo, J., and Costentin, G. (2016). Control of calcium accessibility over hydroxyapatite by postprecipitation steps: influence on the catalytic reactivity toward alcohols. Phys. Chem. Chem. Phys. 18, 27837–27847.
- 40. Diallo-Garcia, S., Ben Osman, M., Krafft, J.-M., Boujday, S., and Guylène, C. (2014).

- Discrimination of infrared fingerprints of bulk and surface POH and OH of hydroxyapatites. Catal. Today 226, 81–88.
- 41. Coenen, K., Gallucci, F., Mezari, B., Hensen, E., and van Sint Annaland, M. (2018). An in-situ IR study on the adsorption of  $CO_2$  and  $H_2O$  on hydrotalcites. J.  $CO_2$  Utilization 24, 228–239.
- Li, X., Lunkenbein, T., Pfeifer, V., Jastak, M., Nielsen, P.K., Girgsdies, F., Knop-Gericke, A., Rosowski, F., Schlögl, R., and Trunschke, A. (2016). Selective alkane oxidation by manganese oxide: site isolation of MnO<sub>x</sub> chains at the surface of MnWO<sub>4</sub> nanorods. Angew. Chem. Int. Ed. 55, 4092–4096.
- Li, X., Teschner, D., Streibel, V., Lunkenbein, T., Masliuk, L., Fu, T., Wang, Y., Jones, T., Seitz, F., Girgsdies, F., et al. (2019). How to control selectivity in alkane oxidation? Chem. Sci. 10, 2429–2443.
- 44. Phivilay, S.P., Roberts, C.A., Puretzky, A.A., Domen, K., and Wachs, I.E. (2013). Fundamental bulk/surface structure–photoactivity relationships of supported (Rh<sub>2</sub>–yCr<sub>y</sub>O<sub>3</sub>)/GaN photocatalysts. J. Phys. Chem. Lett. 4, 3719–3724.
- Phivilay, S.P., Puretzky, A.A., Domen, K., and Wachs, I.E. (2013). Nature of catalytic active sites present on the surface of advanced bulk tantalum mixed oxide photocatalysts. ACS Catal. 3. 2920–2929.
- Uskokovic, V. (2020). X-ray photoelectron and ion scattering spectroscopic surface analyses of amorphous and crystalline calcium phosphate nanoparticles with different chemical histories. Phys. Chem. Chem. Phys. 22, 5531–5547.
- Wu, H., Xu, D., Yang, M., and Zhang, X. (2016). Surface structure of hydroxyapatite from simulated annealing molecular dynamics simulations. Langmuir 32, 4643–4652.
- Cheng, X., Wu, H., Zhang, L., Ma, X., Zhang, X., and Yang, M. (2017). Hydroxyl migration disorders the surface structure of hydroxyapatite nanoparticles. Appl. Surf. Sci. 416, 901–910.
- Wang, X., Zhang, L., Zeng, Q., Jiang, G., and Yang, M. (2018). First-principles study on the hydroxyl migration from inner to surface in hydroxyapatite. Appl. Surf. Sci. 452, 381–388.
- Silvester, L., Lamonier, J.-F., Vannier, R.-N., Lamonier, C., Capron, M., Mamede, A.-S., Pourpoint, F., Gervasini, A., and Dumeignil, F. (2014). Structural, textural and acid-base properties of carbonate-containing hydroxyapatites. J. Mater. Chem. A 2, 11073– 11090
- Veen, H.R.J., Kim, T., Wachs, I.E., Brongersma, H.H., ter Veen, H.R.J., Kim, T., Wachs, I.E., and Brongersma, H.H. (2009). Applications of high sensitivity-low energy ion scattering (HS-LEIS) in heterogeneous catalysis. Catal. Today 140, 197–201.
- Langley, R.A. (2006). Ion scattering spectroscopy in analysis of surfaces. Encyclopedia Anal. Chem. https://doi.org/10. 1002/9780470027318.a2508.
- Baltrusaitis, J., Usher, C.R., and Grassian, V.H. (2007). Reactions of sulfur dioxide on calcium carbonate single crystal and particle surfaces at

- the adsorbed water carbonate interface. Phys Chem. Chem. Phys. 9, 3011.
- Chusuei, C.C., Goodman, D.W., Van Stipdonk, M.J., Justes, D.R., and Schweikert, E.A. (1999). Calcium phosphate phase identification using XPS and time-of-flight cluster SIMS. Anal. Chem. 71, 149–153.
- Tanaka, H., Watanabe, T., and Chikazawa, M. (1997). FTIR and TPD studies on the adsorption of pyridine, n-butylamine and acetic acid on calcium hydroxyapatite. J. Chem. Soc. Faraday Trans. 93, 4377–4381.
- Bolis, V., Busco, C., Martra, G., Bertinetti, L., Sakhno, Y., Ugliengo, P., Chiatti, F., Corno, M., and Roveri, N. (2012). Coordination chemistry of Ca sites at the surface of nanosized hydroxyapatite: interaction with H(2)O and CO. Philos. Trans. A. Math. Phys. Eng. Sci. 370, 1313–1336.
- Hill, I.M., Hanspal, S., Young, Z.D., and Davis, R.J. (2015). DRIFTS of probe molecules adsorbed on magnesia, zirconia, and hydroxyapatite catalysts. J. Phys. Chem. C 119, 9186–9197.
- Sakhno, Y., Bertinetti, L., Iafisco, M., Tampieri, A., Roveri, N., and Martra, G. (2010). Surface hydration and cationic sites of nanohydroxyapatites with amorphous or crystalline surfaces: a comparative study. J. Phys. Chem. C 114, 16640–16648.
- Roy, S., Mpourmpakis, G., Hong, D.-Y., Vlachos, D.G., Bhan, A., and Gorte, R.J. (2012). Mechanistic study of alcohol dehydration on γ-Al<sub>2</sub>O<sub>3</sub>. ACS Catal. 2, 1846–1853.
- Shen, J., Cortright, R.D., Chen, Y., and Dumesic, J.A. (1994). Microcalorimetric and infrared spectroscopic studies of gamma-Al<sub>2</sub>O<sub>3</sub> modified by basic metal oxides. J. Phys. Chem. 98, 8067-8073.
- Hanspal, S., Young, Z.D., Shou, H., and Davis, R.J. (2015). Multiproduct steady-state isotopic transient kinetic analysis of the ethanol coupling reaction over hydroxyapatite and magnesia. ACS Catal. 5, 1737–1746.
- 62. Scalbert, J., Thibault-Starzyk, F., Jacquot, R., Morvan, D., and Meunier, F. (2014). Ethanol condensation to butanol at high temperatures over a basic heterogeneous catalyst: how relevant is acetaldehyde self-aldolization? J. Catal. 311, 28–32.
- Tsuchida, T., Sakuma, S., Takeguchi, T., and Ueda, W. (2006). Direct synthesis of n-butanol from ethanol over nonstoichiometric hydroxyapatite. Ind. Eng. Chem. Res. 45, 8634– 8642.
- 64. Burcham, L.J., Briand, L.E., and Wachs, I.E. (2001). Quantification of active sites for the determination of methanol oxidation turn-over frequencies using methanol chemisorption and in situ infrared techniques. 1. Supported metal oxide catalysts. Langmuir 17, 6164–6174.
- Taifan, W.E.W.E., Bučko, T., and Baltrusaitis, J. (2017). Catalytic conversion of ethanol to 1,3butadiene on MgO: a comprehensive mechanism elucidation using DFT calculations. J. Catal. 346, 78–91.
- Taifan, W.E., Yan, G.X., and Baltrusaitis, J. (2017). Surface chemistry of MgO/SiO<sub>2</sub> catalyst during the ethanol catalytic conversion to

Please cite this article in press as: Kiani and Baltrusaitis, Surface chemistry of hydroxyapatite for sustainable *n*-butanol production from bio-ethanol, Chem Catalysis (2021), https://doi.org/10.1016/j.checat.2021.06.005



### **Chem Catalysis**

Review

- 1,3-butadiene: in-situ DRIFTS and DFT study. Catal. Sci. Technol. 7, 4648–4668.
- 67. Ramesh, K., Ling, E.G.Y., Gwie, C.G., White, T.J., and Borgna, A. (2012). Structure and surface reactivity of WO<sub>4</sub><sup>2-</sup>, SO<sub>4</sub><sup>2-</sup>, PO<sub>4</sub><sup>3-</sup> modified Ca-hydroxyapatite catalysts and their activity in ethanol conversion. J. Phys. Chem. C 116, 18736–18745.
- Moteki, T., and Flaherty, D.W. (2016). Mechanistic insight to C–C bond formation and predictive models for cascade reactions among alcohols on Ca- and Srhydroxyapatites. ACS Catal. 6, 4170–4183.
- Gines, M.J.L., and Iglesia, E. (1998). Bifunctional condensation reactions of alcohols on basic oxides modified by copper and potassium. J. Catal. 176, 155–172.
- Fahmi, A., and Santen, R.A.v. (1997).
   Density functional study of acetylene and
   ethylene adsorption on Ni(111). Surf. Sci. 371,
   53–62.
- Medlin, J.W., and Allendorf, M.D. (2003). Theoretical study of the adsorption of acetylene on the (111) surfaces of Pd, Pt, Ni, and Rh. J. Phys. Chem. B 107, 217–223.
- 72. Müller, P., and Hermans, I. (2017). Applications of modulation excitation spectroscopy in heterogeneous catalysis. Ind. Eng. Chem. Res. 56, 1123–1136.
- Scherzer, M., Girgsdies, F., Stotz, E., Willinger, M.-G., Frei, E., Schlögl, R., Pietsch, U., and Lunkenbein, T. (2019). Electrochemical surface

- oxidation of copper studied by in situ grazing incidence X-ray diffraction. J. Phys. Chem. C 123, 13253–13262.
- 74. Kaya, S., Ogasawara, H., Näslund, L.-Å., Forsell, J.-O., Casalongue, H.S., Miller, D.J., and Nilsson, A. (2013). Ambient-pressure photoelectron spectroscopy for heterogeneous catalysis and electrochemistry. Catal. Today 205, 101–105.
- Landree, E., Marks, L.D., Zschack, P., and Gilmore, C.J. (1998). Structure of the TiO<sub>2-x</sub>(100)-1×3 surface by direct methods. Surf. Sci. 408, 300-309.
- Jehng, J.-M., Wachs, I.E., Patience, G.S., and Dai, Y.-M. (2021). Experimental methods in chemical engineering: temperature programmed surface reaction spectroscopy—TPSR. Can. J. Chem. Eng. 99, 423–434.
- Yashima, M., Kubo, N., Omoto, K., Fujimori, H., Fujii, K., and Ohoyama, K. (2014). Diffusion path and conduction mechanism of protons in hydroxyapatite. J. Phys. Chem. C 118, 5180– 5187
- Petit, S., Thomas, C., Millot, Y., Krafft, J.-M., Laberty-Robert, C., and Costentin, G. (2020). Activation of C—H bond of propane by strong basic sites generated by bulk proton conduction on V-modified hydroxyapatites for the formation of propene. ChemCatChem 12, 2506–2521.
- 79. Horiuchi, N., Nakamura, M., Nagai, A., Katayama, K., and Yamashita, K. (2012). Proton

- conduction related electrical dipole and space charge polarization in hydroxyapatite. J. Appl. Phys. 112, 074901.
- Sans, J.; Arnau, M.; Estrany, F.; Turon, P.; Alemán, C., Regulating the superficial vacancies and OH<sup>-</sup> orientations on polarized hydroxyapatite electrocatalysts. Adv. Mater. Interfaces 2021, n/a (n/a), 2100163.
- Rivas, M., del Valle, L.J., Armelin, E., Bertran, O., Turon, P., Puiggalí, J., and Alemán, C. (2018). Hydroxyapatite with permanent electrical polarization: preparation, characterization, and response against inorganic adsorbates. ChemPhysChem 19, 1746–1755.
- Kasamatsu, S., and Sugino, O. (2018). Firstprinciples investigation of polarization and ion conduction mechanisms in hydroxyapatite. Phys. Chem. Chem. Phys. 20, 8744–8752.
- 83. Prezas, P.R., Melo, B.M.G., Costa, L.C., Valente, M.A., Lança, M.C., Ventura, J.M.G., Pinto, L.F.V., and Graça, M.P.F. (2017). TSDC and impedance spectroscopy measurements on hydroxyapatite, β-tricalcium phosphate and hydroxyapatite/β-tricalcium phosphate biphasic bioceramics. Appl. Surf. Sci. 424, 28–38.
- Al-Hosney, H.A., and Grassian, V.H. (2004). Carbonic acid: an important intermediate in the surface chemistry of calcium carbonate. J. Am. Chem. Soc. 126, 8068–8069.